Applied Design of Corrugated Board Properties to Mitigate Puncturing in Parcel Handling Distribution Chains

Martin Holmvall ,* and Mats Holmgren

*Corresponding author: martin.holmvall@sca.com

DOI: 10.15376/biores.20.3.5377-5397

GRAPHICAL ABSTRACT

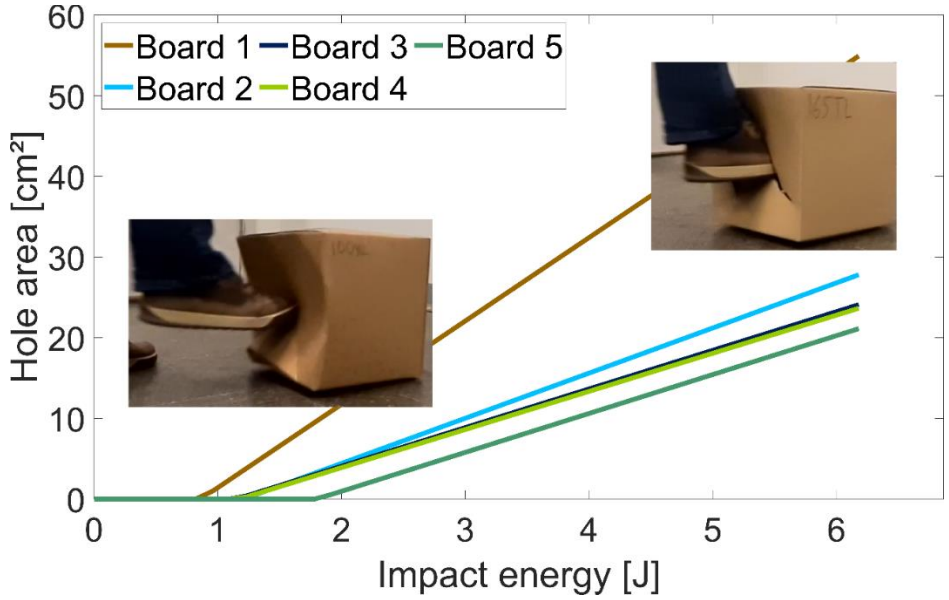

Applied Design of Corrugated Board Properties to Mitigate Puncturing in Parcel Handling Distribution Chains

Martin Holmvall ,* and Mats Holmgren

Corrugated board boxes are used for the majority of parcel shipments. These boxes, particularly in e-commerce shipments, often suffer damages such as crushing and puncturing. Puncture-related damage can lead to product damage, customer dissatisfaction, and costly returns. While holes in boxes due to rough handling in the distribution chain are common, there is no standardized method for designing corrugated board properties to resist puncturing, particularly by selecting appropriate paper materials without extensive laboratory testing. This study demonstrates how commonly measured properties can be leveraged to optimize corrugated board paper combinations, tailoring them to minimize the occurrence of holes, as well as general damage, during distribution.

DOI: 10.15376/biores.20.3.5377-5397

Keywords: Corrugated board; Distribution chain; E-commerce; Parcel; Performance; Puncture; Weibull distribution

Contact information: SCA R&D Centre, Box 716, SE-851 21 Sundsvall, Sweden;
** Corresponding author: martin.holmvall@sca.com*

INTRODUCTION

Millions of parcels are shipped every day worldwide. In 2022, 21.2 billion parcels were shipped in the US alone, and 161 billion globally (Pitney Bowes Inc 2023). For many of these parcels, corrugated board boxes were used as transport packaging. For e-commerce transport packaging, the market share of corrugated board has been estimated to be 80% (Harrod 2019; Smithers 2024). Designing corrugated board boxes involves not only dimensions, features, and visual appearance, but also finding the right material properties to withstand the challenges of the distribution chain. If the necessary material properties and packaging requirements can be achieved in a box, the result should be an intact box and, consequently, safely delivered contents. The primary purpose of each box is to protect its content against the hazards of the distribution chain. Each parcel distribution chain is unique, and within any given chain, no two boxes experience the exact same loading conditions and events, making the design of corrugated board boxes a challenge. In contrast, bulk transporting of boxes stacked on pallets involves a scenario where the bottom box on the pallet is subjected to a known load in a specific direction, for which established design principles exist that largely build upon the box compression strength as a performance parameter (FEFCO 1997; Jönson 1999). For parcel deliveries, no widely accepted principles exist today that aim to mitigate the risk of packaging damage, such as holes. Furthermore, there is no generally accepted performance parameter and design limits to optimize against.

Performance evaluation of boxes began almost immediately after corrugated board boxes became common as transport packaging in the early 1900s (Browder 1935). Around 1910, the burst strength test became the first widely accepted attempt at a performance parameter, driven by the need for safe load limits in railway transport (ISO 2759 (2014)). Although introduced rather arbitrarily and without direct evidence of its relationship to box performance, burst strength has remained in use since then (Coffin 2020).

Rough handling evaluation methods, such as rotating drum tests, were performed at least before 1920, but these kinds of tests are phenomenological in nature and depend on how well they actually describe the actual distribution chain (Anon 1919). Puncturing tests and box compression tests had also been established at this time (Coffin 2020). The puncture test has never been adopted as widely as the burst strength. It has also been questioned by researchers (Jönson 1974; Maltenfort 1989; Steadman 2002). The box compression test, on the other hand, is well established and suited for palletized transports and stacked storage. Box compression is also relevant to parcel deliveries, in which boxes can be simultaneously subjected to compressive loads, vibrations, and shocks (Lamb and Rouillard 2017; Molnár and Böröcz 2021; Mrówczynski *et al*. 2023). However, stacked box transports, whether on pallets or as parcels, do not cause holes in the boxes. Since unintended drops are well-known events in parcel deliveries, several drop tests have been developed. Early studies by Kellicutt *et al*. found a relationship between the height of a single drop on a box corner causing box failure, the burst strength, and the content weight (Kellicutt and Landt 1951; Kellicutt and Landt 1956; Kellicutt 1960a,b). But, these results were achieved without connection to distribution chain data and were dependent on flute type, which was not captured by the burst strength value. This flute type dependence was also later observed by Batelka (1994). A study by Buchanan involved testing boxes filled with either cans or cartons of powder shipped within England (Buchanan 1967). The transportation involved delivery vans combined with either railways or truck trailers, and the damage to the boxes and their contents was evaluated using a predetermined protocol. The study concluded that for boxes filled with cartons, a seven-drop test in various orientations best correlated with the damages. For boxes filled with cans, the burst strength test demonstrated the highest correlation. In this study, limited information about the distribution chain was provided, with details only about the types of vehicles used, distances traveled, and storage durations.

Another notable study by Jönson involved corrugated board boxes containing tin cans, cardboard cartons, and vacuum cleaners (Jönson 1974). Shipments were conducted both within Europe and on a route to the USA. Jönson developed a protocol to evaluate packaging damages resulting in a combined damage coefficient. The study concluded that the edge crush test value and burst strength were crucial properties for reducing damage, especially edge crush. However, no single property was universally decisive.

Today, the most common approach to designing boxes and materials for parcel deliveries involves the use of standardized transport test protocols (ISTA 3B 2017; ISTA 3A 2018; ISTA 6-Amazon 2018; Böröcz and Németh 2025). These protocols serve to simulate real-world distribution chain events that can harm a box and its content, usually evaluated by inspection. Capturing the complexity of real-world distribution in laboratory tests is, however, a challenge and important aspects are often overlooked (Rouillard *et al*. 2021).

Summarizing the available literature, there exist various field trials, lab tests, and standardized test protocols related to box or content damage. Still, there is a lack of systematically quantified scalar data related to box damage evaluations, in combination

with scalar data representing the distribution chain, which are necessary for optimizing calculations with high accuracy. In contrast, extensive distribution chain data exists within the closely related field of packaging research, focusing on vibrations and shocks during transport (Singh *et al.* 2010; Böröcz and Németh 2025). This data defines and classifies the distribution chain using tools such as accelerometers but focuses primarily on content and cushioning needs rather than the performance of the box material to prevent damage.

This work focuses on optimizing corrugated board in boxes to prevent holes in the panels. The optimization process involves mapping the parcel distribution chain using accelerometers to obtain transport test data, from which a key parameter, denoted as the characteristic drop height, is identified. In combination with a previously published equation that describes the relationship between the size of a hole generated in a corrugated board panel and the energy absorbed by the material upon penetration, the characteristic drop height can be used to design corrugated board box materials (Holmvall *et al*. 2024). This method allows for selecting suitable paper combinations for corrugated board based on characteristic drop height, box panel area, and standard paper properties, enabling tailored box materials without time-consuming transport test protocols or corrugated board measurements.

EXPERIMENTAL

Box Materials

Five corrugated board materials were selected for the transport test. The properties of the corrugated boards and the corresponding containerboards are presented in Tables 1 and 2, respectively.

Table 1. Corrugated Board and Corresponding Box Properties

Board grade	Liner Composition (outer/fluting/inner)	Takeup (-)	Burst (kPa)	ECT (kN/m)	DST (bpi)	BCT without insert (kN)	BCT with insert (kN)
$85HF_{CB}$	85HF/85HF/85HF - R	1.26	467	3.9	3.5	1.02	3.16
$160TLW_{CB}$	160TLW/110HF/160TLW - B	1.26	774	5.1	7.9	1.66	4.48
$135KT_{CB}$	135KT/120HF/165TL - B	1.33	743	6.0	10.8	2.51	4.88
$165TL_{CB}$	165TL/120HF/165TL - B	1.33	755	7.1	11.5	2.05	4.88
$150KL_{CB}$	150KL/130HF/150KL - R	1.22	1273	6.7	8.3	2.36	4.79

Table 2. Containerboard Properties

Paper grade	Basis weight (g/m^2)	$\overline{TEA}$ (J/m^2)	$\bar{\sigma}_{max}$ (kN/m)	$\bar{S}_t$ (kN/m)
85HF	85	61	3.55	420
110HF	110	73	4.47	540
120HF	120	98	5.39	610
130HF	130	69	4.61	561
135KT	135	126	6.16	667
150KL	150	195	9.74	885
160TLW	160	137	6.46	712
165TL (with 135KT)	165	110	6.48	770
165TL (outer, symmetric)	165	121	6.36	738
165TL (inner, symmetric)	165	97	6.40	780

The materials were selected from single-wall corrugated boards commonly used for e-commerce packaging by the manufacturer. The primary selection criterion was to represent a broad performance range, achieved by including a low-basis-weight fluting paper at the lower end and a virgin fiber kraftliner-based corrugated board at the higher end.

Geometrical mean values from measurements in the machine direction (MD) and cross machine direction (CD) are denoted by a bar over the parameter. The classification and nomenclature of the paper grades follow the CEPI standard, where applicable (CCB 2022). All papers are designated by their basis weight and a paper grade abbreviation, such as 150KL for a kraftliner with a basis weight of 150 g/m², and 165TL for a testliner with a basis weight of 165 g/m². Other abbreviations used include HF for high-performance recycled fiber-based fluting papers, KT for kraft-top liner, and TLW for white top testliner. Corrugated boards are denoted by their liner grades with the subscript "CB". All corrugated boards are symmetrical, except one where the outer liner is a kraft-top liner, and the inner liner is a testliner. In the transport test, standard FEFCO 0201 boxes (also called regular slotted container (RSC)) were used with internal dimensions of 275×275×195 mm. Structural inserts were placed inside each box to maintain its shape during distribution and to enhance protection against compressive damage (see Figs. 1A and 1B). These inserts were designed to ensure that the side panels could absorb impact energy without interference but simultaneously preventing the box structure from mitigating impact effects on the panels by deforming the box. Additionally, the inserts were configured to house a smaller box for securing an MSR175 plus accelerometer, which recorded events along the distribution chain (see Fig. 1C) (MSR175_plus 2025). The accelerometer sampled events at a frequency of 6400 Hz with the 200g option. The yellow accelerometer was tightly encased to prevent any internal movement. The total weight of the boxes was 1.4 kg.

Distribution Chain

The transport test involved shipping boxes from the SCA R&D Centre in Sundsvall, Sweden, to an address in Stuttgart, Germany. This corresponds to a linear distance of approximately 1600 km or a road distance of around 2000 km. For the outbound trip, the boxes were shipped *via* DHL Express. For the return trip, ordinary DHL shipment was used. The primary difference between DHL Express and ordinary DHL delivery was that DHL Express transported the boxes by truck for approximately 340 km to an airport, from which they were flown to Germany. Conversely, the return trip *via* ordinary DHL involved truck transport for the entire route from Stuttgart to Sundsvall. Upon arrival in Stuttgart, the boxes were inspected for damage according to a protocol developed by Jönson (1974). On their return to the SCA R&D Centre, the boxes were inspected again using Jönson's protocol. The accelerometers placed inside the boxes were retrieved and the data recorded was analyzed. A total of 10 boxes were sent in each shipment (see Fig. 1D), two from each corrugated board grade, with a total of 10 shipments conducted from December 2023 to May 2024. Due to turnaround time constraints, only seven shipments included accelerometers. Some boxes were excluded from the evaluation because they had been cut open during customs clearance. As a result, between 18 and 20 boxes from each material were used for damage evaluation.

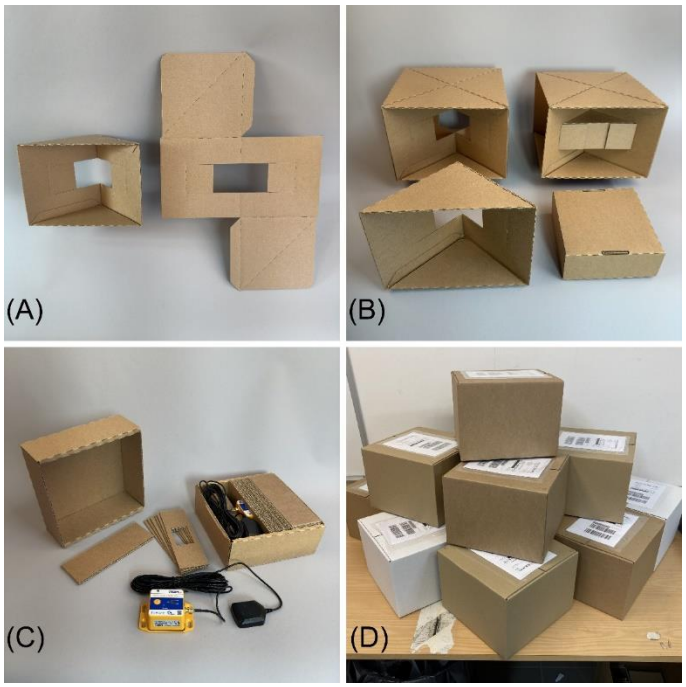

Fig. 1. Corrugated board box configuration for the transport test. (A) A quarter of the final insert (flat sheet and folded structure) with a hole for the accelerometer box. (B) Four insert quarters are glued together and the box with the accelerometer is glued in the center of the insert. (C) A lid and bottom box with the accelerometer in the center including GPS antenna. The accelerometer is tightly secured with tailor-cut corrugated board pieces. (D) A shipment batch of ten boxes made from five different corrugated board materials. All inserts were made using the corrugated board denoted $150KL_{CB}$.

Damage Evaluation

The damage evaluation protocol described by Jönson (1974) includes the following criteria:

Damage report components:
- Type of damage
- Location of the damage
- Size of the damage

Type of damage classification:
- A – Completely undamaged box
- B – Abrasive damage
- C – Damage that does not deform shape
- D – Damage that deforms shape
- E – Punctured

Location of damage classification:
- Top
- Bottom
- Edge
- Side
- Corner

According to Jönson (1974), the size of the damages should be classified into size ranges; however, the present study did not categorize damage size. To enable evaluation and comparison, types and locations of damage were assigned coefficients based on the estimated severity of the damage. The coefficients were established by Jönson in collaboration with both producers and vendors. Essentially, these coefficients increase with the risk of damage to the content. The higher coefficient for puncture damage compared to shape deformation can be justified by the fact that a deformed box primarily poses a risk to fragile items, such as electronics, but it is less critical for non-fragile items like clothing. Puncture damage, however, is hazardous to both fragile and non-fragile items, as it adds the risk of contamination or tampering. The evaluation coefficients for a corrugated board box are detailed in Tables 3 and 4.

Table 3. Coefficients for Different Types of Transport Damages on Boxes

Type of damage	Coefficient
A – Undamaged	0
B – Abrasive damage	1
C – Damage without shape deforming	5
D – Damage that deforms shape	10
E – Puncturing damage	20

Table 4. Coefficients for Different Locations of Damages on Boxes

Location	Coefficient
Top	0.1
Bottom	0.1
Side	0.5
Edge	1.0
Corner	0.5

Because the aim of this work was to validate a material design equation developed for single-wall corrugated board, damages located on the top and bottom of the boxes were not included in the evaluations. The tops and bottoms of the box contain two layers of corrugated board in the chosen design, which interferes with the assumptions of the equation. The damage coefficient (DC) for a box is calculated using Jönson's equation,

$$DC = \sum_{i=1}^{5} \sum_{j=1}^{5} P_i Q_j N_{ij} \quad (1)$$

where P_i is the damage type coefficient from Table 3, $Q_j$is the location coefficient from Table 4, and N_{ij} is the number of damages combining type i and location j. The final damage coefficient can then be used to compare the level of damage between boxes and materials.

Design Equation

The design equation proposed by Holmvall *et al*. (2024) describes the relationship between the energy absorbed (E_{ABS} (J)) by a corrugated board panel when it is penetrated by an impacting object creating a hole with an area A_{obj} (m²). The absorbed energy comprises several components: the energy involved in rupturing the papers (E_R (J)), straining of the corrugated board liners (E_S (J)), and crushing of the flutes (E_C (J)). Additionally, according to Holmvall *et al*. (2024), for blunt objects, a friction-related

correctional term needs to be added to account for the difference between corrugated board corners and the smooth steel hemisphere used in the development of the equation. Thus, the total absorbed energy is the sum of these components, as described by the following equation,

$$E_{ABS} = E_R + E_S + E_C + 0.5 \quad (2)$$

Equation 2, detailed by Holmvall *et al*. (2024), can be used to calculate a "puncture threshold," *i.e.*, an energy limit below which no holes are created upon impact with an object. If no hole is created at impact, then there will be no rupturing of the papers and no crushing of the flutes, but the correction term is still necessary since it is needed to adjust the level. Thus, Eq. 2 can be written as follows,

$$Puncture\ threshold = $$
$$= 0.23\left(\left(\frac{\bar{\sigma}^2_{close}}{2\bar{S}_{t,close}}\right) + \left(\frac{\bar{\sigma}^2_{opp}}{2\bar{S}_{t,opp}}\right)\right)A_{panel} + 0.5. \quad (3)$$

where $\bar{\sigma}$ (N/m) represents the geometric mean of the tensile strength of the corrugated board liners. The subscripts "*close*" and "*opp*" indicate whether the liner is closest to or opposite the impacting object. $\bar{S}_t$ (N/m) denotes the geometric mean of the tensile stiffness of the liners, and A_{panel} (m²) is the area of the impacted corrugated board panel of the box.

Equation 2 is derived under the assumptions of a blunt impactor, a center panel strike, and a normal (perpendicular) impact. However, when the impact does not result in puncture—as is the case at or below the puncture threshold—the specific impact shape or angle becomes less critical. Impacts occurring near the panel edges may still produce punctures even at or below the nominal threshold, due to reduced deflection capacity at the edges compared to the center. Conversely, in real-world conditions, impacts near the edges are more likely to induce rotation of the box away from the point of contact, which can dissipate part of the impact energy and reduce the likelihood of puncture. For the purpose of designing corrugated boards to resist puncture in parcel distribution chains, the blunt-object formulation of Eq. 2 is deemed appropriate. Holmvall *et al*. (2024) demonstrated that fresh (*i.e*., non-indented) box corners made of corrugated board can be reasonably modeled as blunt impactors when selecting between the sharp and blunt versions of Eq. 2. Objects that are significantly sharper and harder than this are considered anomalies within the distribution chain and are therefore excluded from the design criteria.

RESULTS AND DISCUSSION

Damage Evaluation

The damage evaluation was conducted by two independent observers. Figure 2 displays the average damage coefficients for all evaluated boxes and each box material. The coefficient of variation for Observer 1 in Stuttgart ranged from 31% to 55%, whereas for Observer 2 at the SCA R&D Centre, it was between 16% and 25%. Although these variations are relatively high, it is important to remember that shipment conditions differ from controlled laboratory tests. During parcel transport trials, some boxes may encounter extreme conditions in one shipment but not in others. Therefore, it is crucial to ship a sufficient number of boxes to obtain stable average values. Observer 1 reported lower damage coefficients compared to Observer 2; however, the ranking of different box

materials remained consistent. A lower damage coefficient indicates a less damaged box. The high coefficient of determination (r^2 = 0.97) between the halfway evaluation in Stuttgart and the final destination Sundsvall suggests that, on average, rough handling shipment damages progressively accumulate along the distribution chain. Moreover, the degree of damage is consistent with the properties of the box materials.

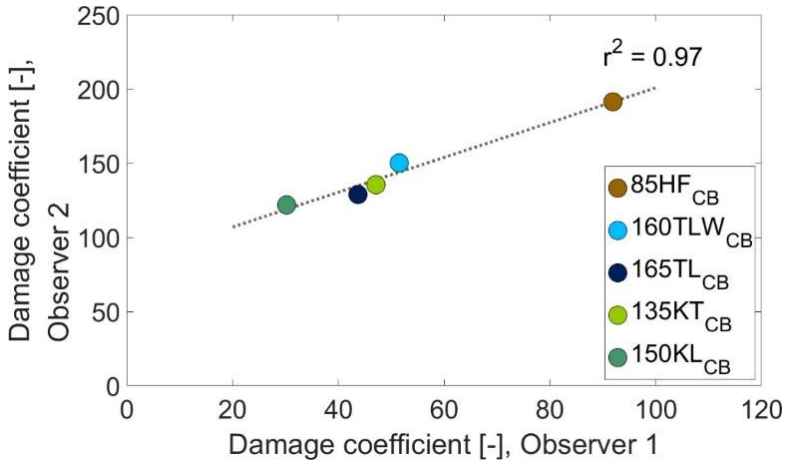

Fig. 2. The average damage coefficients for the boxes, as evaluated by Observer 1 in Stuttgart, Germany, and Observer 2 at the final destination in Sundsvall, Sweden, indicate that the damages accumulate according to the material properties throughout the distribution chain.

Figure 3 gives an overview of the shipped boxes. For each material, 16 transported boxes are shown. For each box, the side panel showing the most damage is facing the camera. Boxes made from $85HF_{CB}$ sustained more deforming damages and larger holes in general. The $160TLW_{CB}$, $165TL_{CB}$ and $135KT_{CB}$ boxes had fewer damages, and the $150KL_{CB}$ boxes appeared almost unharmed, with only slight deformations or minor dents.

Damage Data Analysis

When choosing the material for a box to meet specific performance levels for parcel distribution chains, the box's compressive strength is often evaluated as a performance parameter. This strength is tested both with and without content, using static methods and vibrational tables (ISTA 3B 2017; ISTA 6-Amazon 2018). One prevalent standard test for box strength is the Box Compression Test (BCT) (FEFCO 1997). This test measures the top-to-bottom compressive strength of a box and is primarily used for vertically loaded boxes such as those stacked on pallets. BCT tests are not intended to evaluate the risk of puncture, but the tests are often used as a general rough handling parameter in box design for a variety of applications, such as e-commerce boxes. Burst strength, another parameter widely used, characterizes the ability of a corrugated board material to withstand one type of penetrative damage. Figure 4 illustrates the correlation of both BCT with and without inserts and the burst strength to the damage coefficient. The BCT values for boxes with inserts, as the boxes that were shipped, showed the highest correlation. BCT values for empty boxes had a lower correlation and burst strength a poor correlation. It is reasonable that measuring of boxes in the same configuration as they were shipped best correlates to the degree of damage, but it also indicates that the combined packaging compressive strength is a significant parameter also for parcel shipments. Unfortunately, there is no simple way to determine what would constitute a limiting box strength to optimize against, based on distribution chain data.

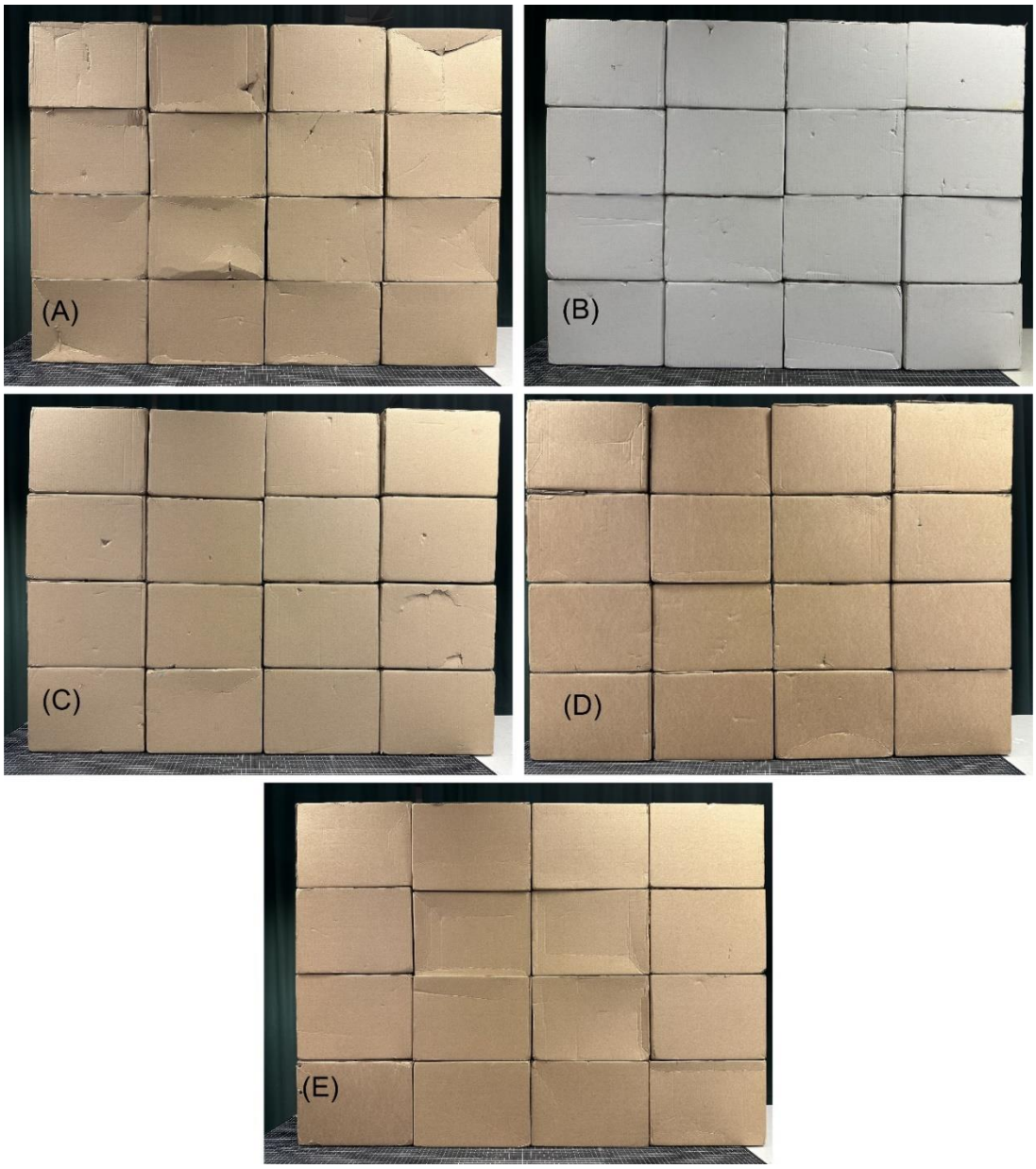

Fig. 3. Visual appearance of the boxes after the transport test. The photos show the 16 most damaged boxes for each material, with the most damaged side panel facing the camera. (A) 85HF$_{CB}$, (B) 160TLW$_{CB}$, (C) 165TL$_{CB}$, (D) 135KT$_{CB}$, and (E) 150KL$_{CB}$

Analyzing the construction of the damage evaluation protocol in the Damage Evaluation section and the weighting of coefficients in Table 3 for different types of damages, it can be concluded that holes are regarded as more severe than, for instance, compressive damages. This intentional weighting by Jönson reflects the perception that holes pose a greater threat to the primary function of a box, which is to protect its contents. While the burst test does measure a penetration property, it is a quasi-static measurement with limited contribution from the fluting. This is significant because fluting has been shown to play a crucial role in preventing ruptures during dynamic impacts (Holmvall *et al*. 2024). As Fig. 4 shows, the burst strength does not capture the protective performance of the materials that well.

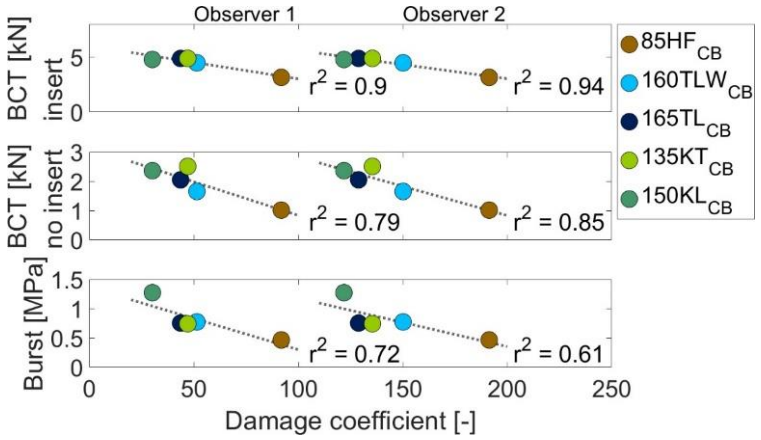

Fig. 4. Commonly measured parameters for corrugated board and boxes to optimize boxes for parcel delivery. The BCT was measured both with and without the inserts shown in Fig. 1. The damage coefficients by Observer 1 is to the left and Observer 2 to the right. In all cases, the standard deviation of the parameter is less than the size of the marker.

To address this, an alternative approach was employed to correlate a parameter with the damage coefficients. By assuming that rough handling in the distribution chain can be represented by an artificial free-fall drop height and a corresponding level of potential energy, the resulting hole area can be calculated using Eq. 2, based on the material properties listed in Table 2. Figure 5 displays the calculated values for all corrugated board materials in Table 1 based on three arbitrarily chosen drop heights: 15, 25, and 35 cm. These calculations were made for a box with a total weight of 1.4 kg and a side panel area of 0.054 m², matching the weight and size of the boxes used in the transport trial. As shown in Fig. 5, the correlation between hole area and damage coefficient, evaluated using the coefficient of determination, was high for both sets of observer damage coefficients – even higher than for the measured box strength for boxes with inserts. This correlation remained strong regardless of the chosen drop height. These results indicate that the paper properties used to calculate an impact hole area, using Eq. 2, provide a better basis for assessing the potential level of damage a parcel receives in the distribution chain compared to burst strength and BCT.

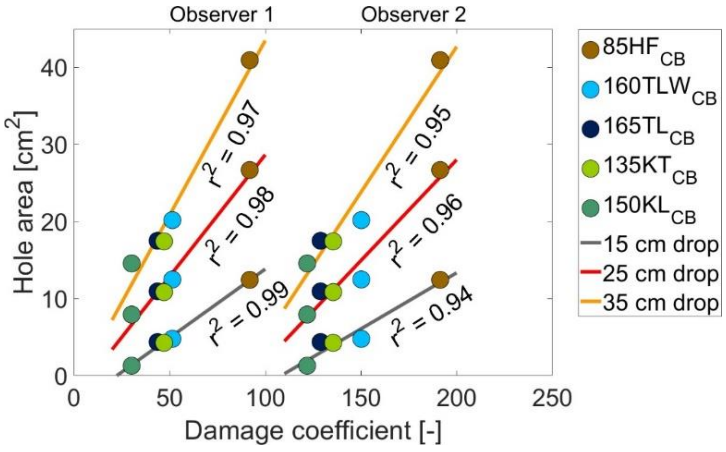

Fig. 5. The calculated hole area versus the damage coefficients from the transport trial. The calculations were performed assuming three example drop heights, which were converted to the free fall potential energy for a 1.4 kg box.

It should be noted that, while the strong correlation between hole area and damage coefficient may partially originate from the emphasis on holes in Jönson's damage evaluation protocol, the protocol is designed for general damage evaluation of boxes, such as those shown in Fig. 3. One conclusion that can be drawn from Fig. 5 is the invariance of correlation with respect to where in the distribution chain the evaluation was made (represented by the consistency in results between the two observers), as well as the assumed harshness level of the distribution chain (represented by the drop height). This suggests that Eq. 2 can be used to improve corrugated board for parcel deliveries without needing detailed information about the parcel distribution chain. The equation ranks and scales as the damages regardless. However, without knowing a unique artificial drop height representative of the distribution chain, it is not possible to optimize against a known limit where damages are minimized.

Corrugated Board Optimization

To establish a representative distribution chain drop height and, more specifically, to find a limit suitable for corrugated board optimization, the data from the accelerometers was analyzed. An acceleration threshold of 3 g was necessary to avoid the accelerometer memories becoming filled up before returning to SCA R&D Centre. One roundtrip generated in the order of 1000 recorded shocks above 3 g, but the variation was large. Figure 6 shows the cumulative distribution function (CDF) for peak acceleration of one roundtrip with ten boxes in which two boxes were made from each of the materials in Table 1.

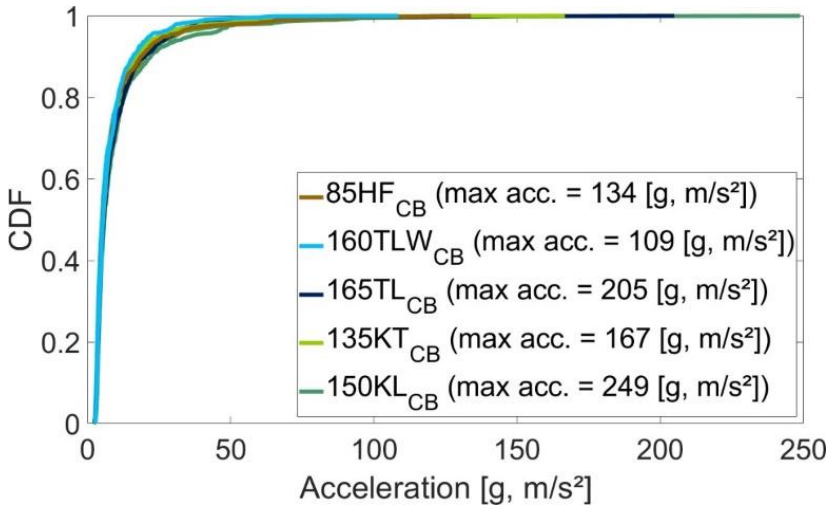

Fig. 6. The cumulative distribution function for the peak accelerations (in the direction of the acceleration vector) for all recorded events during one roundtrip of the transport trial

The CDF curves shown in Fig. 6 are similar to each other for all materials. Some boxes recorded some accelerations outside of the working range of the accelerometer, but there were only a handful of such recordings. The largest difference between the materials was for accelerations below 50 g. Therefore, Fig. 6 is replotted in Fig. 7 to more clearly show the difference between curves.

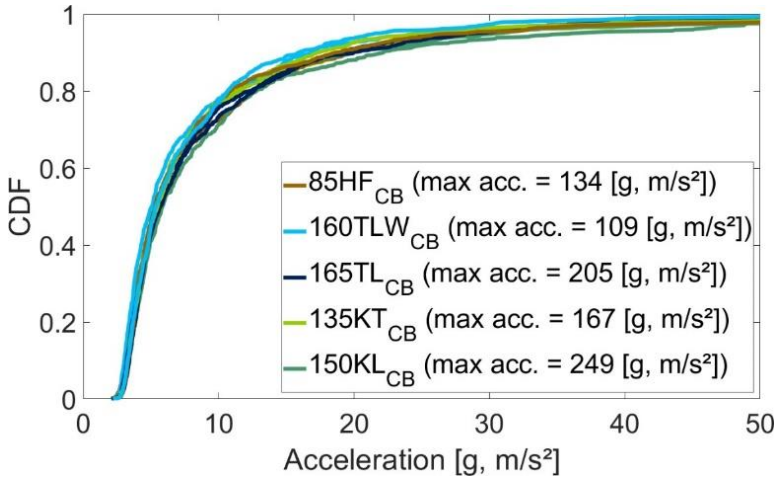

Fig. 7. The cumulative distribution function for the peak accelerations in the range up to 50 g

In Fig. 7 the 3 g acceleration threshold is visible as the shift of the CDFs from zero to the right. Although the curves may appear similar, the actual difference between the same material CDFs can be as large as 0.1 or more for some accelerations, which is thought to be a significant difference for the current purpose. Therefore, all roundtrips for which the accelerometers were recording were added into one distribution for each material. The result can be seen in Fig. 8. For each material, all recorded impact events for the different shipments have been treated as one shipment. This is done for each of the materials and each curve represents between 5520 to 8615 recorded events. As Fig. 8 shows, there was no longer any significant difference between the materials. Therefore, the conclusion was that there was no significant difference between the boxes in impact circumstances due to the way of transport, box material, or ambient conditions. That is, the CDFs seem to have represented the distribution chain well and that the amount of data were sufficient.

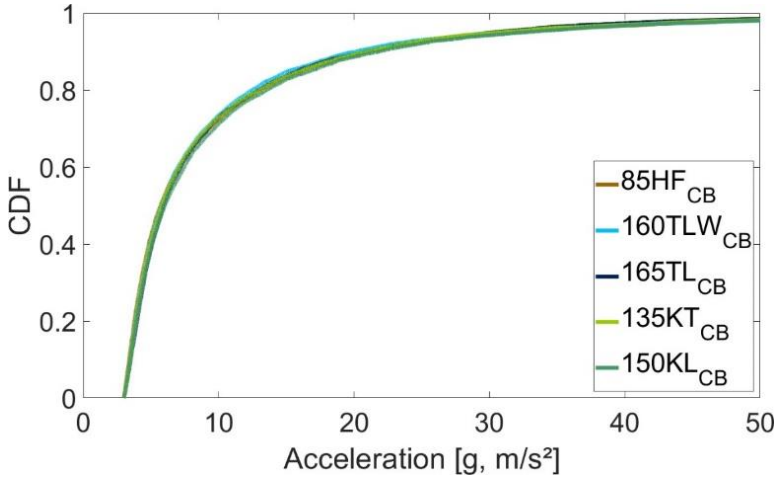

Fig. 8. The CDFs from all shipments combined into one CDF for each material. The curves for different materials are on top of each other.

The next step was to convert the accelerations into corresponding drop heights. This is necessary to enable calculations with Eq. 2. To do this, two assumptions need to be made. Firstly, Eq. 2 is based on an idealized case where a box side panel is impacted in the center by a free-falling blunt object in the normal direction to the panel. This is not the case for

actual field trials, as Fig. 3 shows. But, since the aim is not to correctly calculate the hole area for each impact, but rather finding a drop height that represents all holes created through the entire distribution chain, it is only necessary that there exists a proportionality between the effects from the actual impacts, regardless of impact direction, or position of the hit on the panel, and the ideal case. It is to be expected that the properties governing the hole size in the center of a panel is also the same at other positions on the panel. Secondly, it is assumed that a representative drop height can be found from the peak accelerations instead of with the constant accelerations from which the kinematic equations are derived. Again, it is assumed that proportionality is sufficient, which should be the case with approximately symmetrical and similar first impact peak curves as in Holmvall *et al*. (2024). The conversion is derived by the usual conservation of energy from an initial drop height, *h*,

$$\frac{mv^2}{2} = mgh \xrightarrow{yields} v^2 = 2gh, \quad (4)$$

where m (kg) is the mass of the object, v (m/s) is the velocity, and g (m/s²) is the gravitational acceleration constant. Combining Eq. 4 with the kinematic relationship, shown in Eq. 5,

$$a = \frac{v^2}{2d} \quad (5)$$

introducing the constant acceleration, a (m/s²), the distance the acceleration acts, d (m), and also converting to g-forces by Eq. 6,

$$g\text{-}force = \frac{a}{g} \quad (6)$$

results in Eq. 7,

$$g\text{-}force = \frac{h}{d}. \quad (7)$$

Although Eq. 7 is derived under simplified assumptions, it serves as a valid first-order approximation. In real-world scenarios, impacts typically involve both translational and rotational motion of one or both bodies, contributing to the total kinetic energy of the system. Additionally, rotational and vibrational components are a part of the recorded accelerations shown in Fig. 8, thereby violating the idealized conditions under which Eq. 7 was derived. However, most recorded events do not represent pure free-fall impacts. Rather, they involve complex interactions such as boxes colliding with other boxes, surfaces, or being handled during transport. The primary purpose of Eq. 7 is to convert measured accelerations into an equivalent potential energy, represented as an apparent drop height. Provided that rotational and vibrational accelerations contribute approximately proportionally to the translational accelerations across the dataset shown in Fig. 8—as assumed—this approximation remains suitable for establishing an optimization threshold since it will be calibrated to represent the distribution chain.

Equation 7 can be used to transform the acceleration data in Fig. 8 to free fall drop heights if the distance over which the acceleration acts is known. Therefore, an experiment was performed with drops from known heights and the box landing flat on the bottom panel, avoiding rotational effects as much as possible as the box hit the floor. The result is shown in Fig. 9.

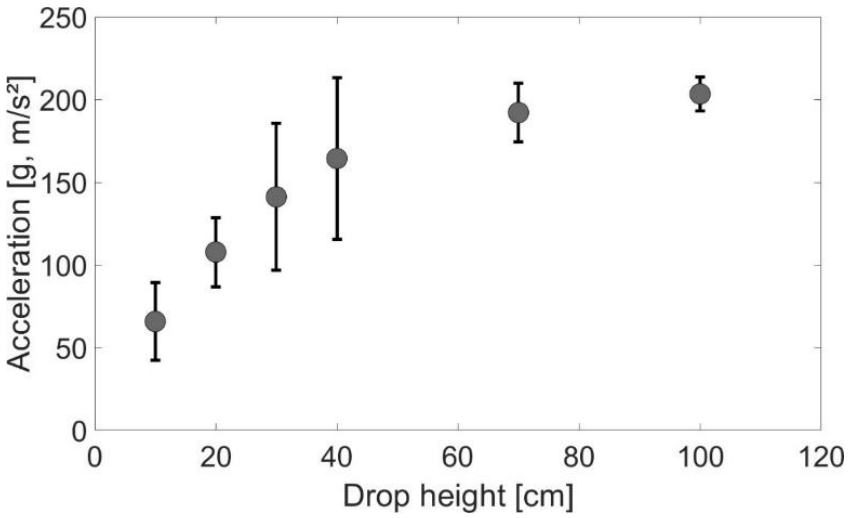

Fig. 9. Peak accelerations for transport trial boxes dropped flat-bottomed onto a concrete floor

From Fig. 9 and Eq. 7 the apparent distance over which the acceleration acts were calculated. A linear interpolation was used in Fig. 9 to find intermediate values. For accelerations above 200 g, the highest drop height result was used. In Fig. 10, the peak accelerations have been converted into free fall drop heights.

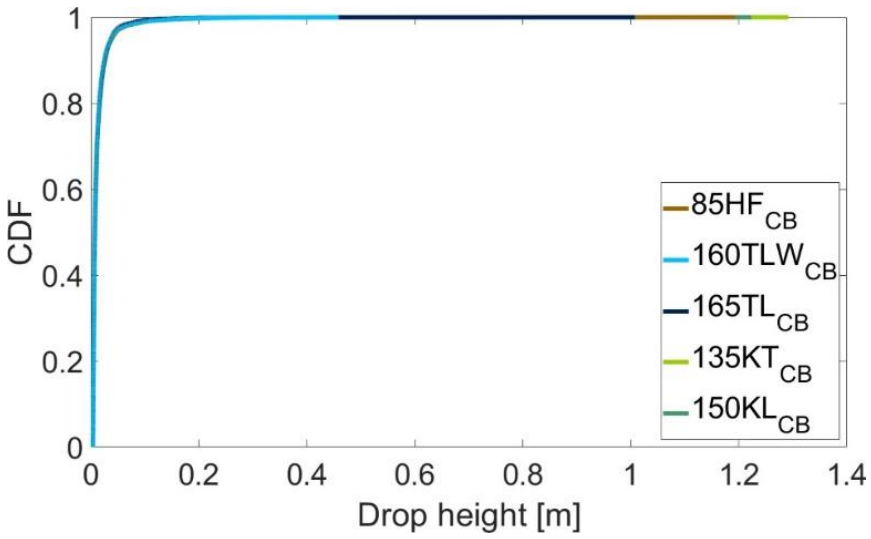

Fig. 10. The CDF of apparent drop heights from the transport trial. The difference in maximum drop height of the curves corresponds to the highest recorded acceleration as in Fig. 6, but for all roundtrips.

To accommodate direct calculations with the CDF, a curve fit was performed, but interpolation could also have been employed. The data were fitted to a three parameter Weibull distribution. The Weibull distribution was chosen for convenience, and no consideration was made as to whether it is an accurate description of the process. However, the Weibull distribution has been used before to model distribution chain data in the field of vibrations analysis (Böröcz 2018; Rouillard and Lamb 2020). The Weibull parameters are presented in Table 5.

Table 5. Weibull Parameters Fitted to the Experimental CDFs of Drop Heights

Material	*B*, shape	*η*, scale (m)	*γ*, location (m)	No. recorded events	Nonlinear rank regression R^2
$85HF_{CB}$	0.690174	0.006915	0.003611	6656	0.98
$160TLW_{CB}$	0.710876	0.006914	0.003612	7948	0.98
$135KT_{CB}$	0.710774	0.007034	0.003612	8615	0.98
$165TL_{CB}$	0.738812	0.007195	0.003612	5520	0.98
$150KL_{CB}$	0.709248	0.00754	0.00361	6919	0.97

In Fig. 11, the puncture thresholds, calculated using Eq. 3, are shown for each material. The corresponding drop heights were found by recalculation of the puncture threshold energies using the potential energy of a free-fall using a mass of 1.4 kg. The dotted lines in Fig. 11 are drawn from the drop heights of the puncture threshold up to the CDF value calculated with the fitted Weibull parameters. The CDF values are close to 1 at the puncture thresholds, but the differences between the calculated CDF values and 1 that do exist are usually called the probability of survival. For the purpose of this work, this is a misleading denomination, and it is therefore in this work denoted as the probability of damage. According to Eq. 3, a puncturing damage occurs above the puncture threshold.

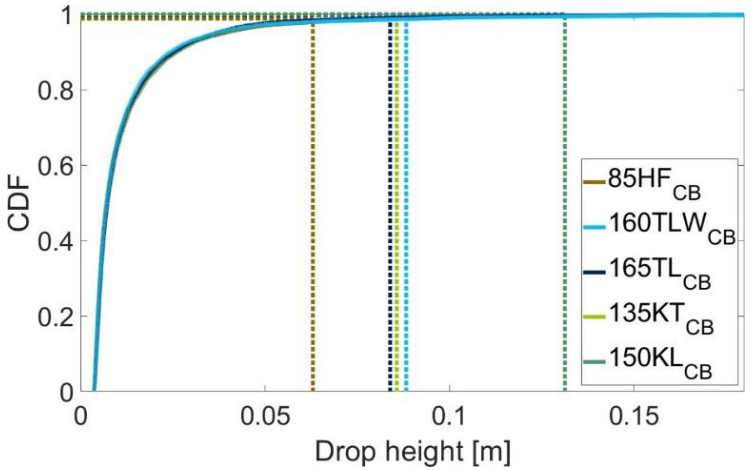

Fig. 11. The CDF of apparent drop heights as solid lines and with the corresponding puncture thresholds calculated with Eq. 3 for each material converted into a free fall drop height and illustrated as dotted lines

The probability of damage values were used to establish an apparent drop height that could represent the rough handling in the distribution chain. This representative drop height is denoted the characteristic drop height. The first step to find the characteristic drop height for a distribution chain is to calculate the hole area with Eq. 2 for all relevant drop heights. Figure 12 shows the results in the same drop height range as in Fig. 11. As Fig. 12 shows, every curve determined in that way had an initial flat range equal to zero. This is the range from zero drop height up to the puncture threshold drop heights shown in Fig. 11. After that, with higher drop heights, the hole area increased linearly. The reasoning is that the average sum of hole areas on a box (in this case the total hole area per box on its four side panels) can be represented by a single drop height for that material. With Eq. 2 it

is always possible to find a specific drop height, corresponding to any hole size larger than zero, for any single wall corrugated board material. This drop height yields a hole area which, in turn, must be proportional to the probability of damage, since the probability of damage will be proportional to the accumulated hole area above the puncture threshold drop height for that material. The proportionality is guaranteed by the linearity of the hole area above the puncture thresholds. The step to defining the characteristic drop height for a material is then a question of finding the drop height that generates hole areas that align for all materials and the specific distribution chain.

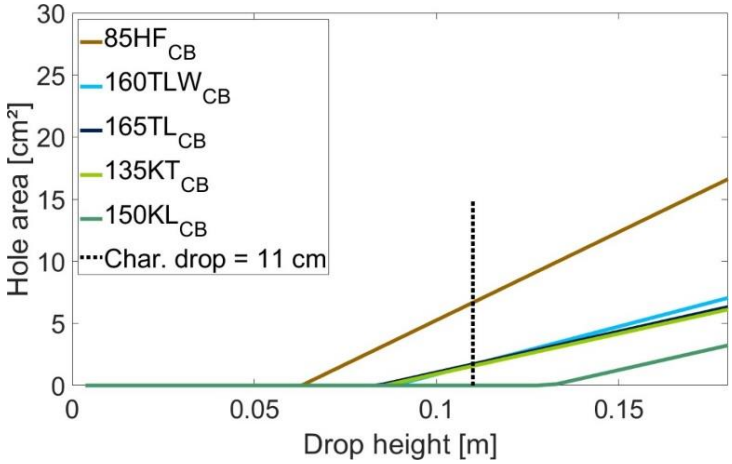

Fig. 12. The hole area calculated with Eq. 2 for the materials in Table 1 as well as the drop heights in Fig. 11. An example of a characteristic drop height is shown as a dotted black line.

Figure 13 shows how the characteristic drop height can be identified. The hole areas for a single drop height are calculated for each material and plotted against the probability of damage corresponding to each material. The drop height the regression line of which is closest to cross the origin is set as the characteristic drop height. The hole area should be zero when the probability of damage is zero. Therefore, the characteristic drop height is 11 cm for the distribution chain from SCA R&D Centre in Sweden to Stuttgart, Germany and back.

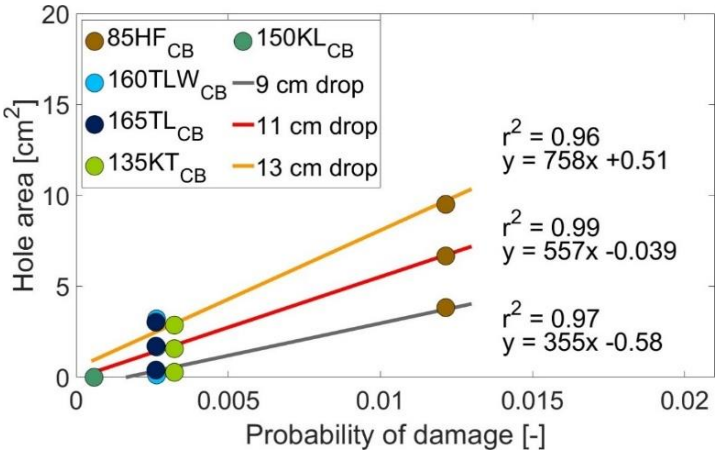

Fig. 13. Calculated hole areas plotted against the probability of damage for three different drop heights. The linear regression line closest to go through the origin yields the characteristic drop height. In this case 11 cm.

The purpose of establishing the characteristic drop height is that it can be calculated into a free-fall potential energy using the package weight, yielding the limit against which Eq. 3 can be optimized, to minimize puncturing holes for the distribution chain in question. That is, the puncture threshold for a material should be larger than the free-fall characteristic drop height potential energy of the distribution chain.

To verify the use of the probability of damage parameter and the Weibull curve fit, the number of holes in the four side panels of the boxes were counted. With enough shipped boxes, the relative fractions of the average number of holes per box should be proportional to the probability of damage for boxes of that material. In Fig. 14, the calculated hole areas for three different drop heights are plotted against the average number of holes per box, just as in Fig. 13. In this case, the data for the $150KL_{CB}$ box were omitted because Eq. 2 predicts that no holes should occur for those boxes at the drop heights used for the calculations. Including this data would interfere with the linear regression. This is evident from Fig. 12, where the characteristic drop height was well below the puncture threshold for $150KL_{CB}$. Including that data point for all drop heights would erroneously skew all lines towards zero. It is always best to conduct the characteristic drop height calibration with materials that have a hole size larger than zero for all drop heights in the calculation.

As Fig. 14 shows, using the average number of holes as a measure of the severity of the distribution chain, the 11 cm drop height was the one closest to zero, defining the characteristic drop height. This supports the method of using the probability of damage as a defining parameter.

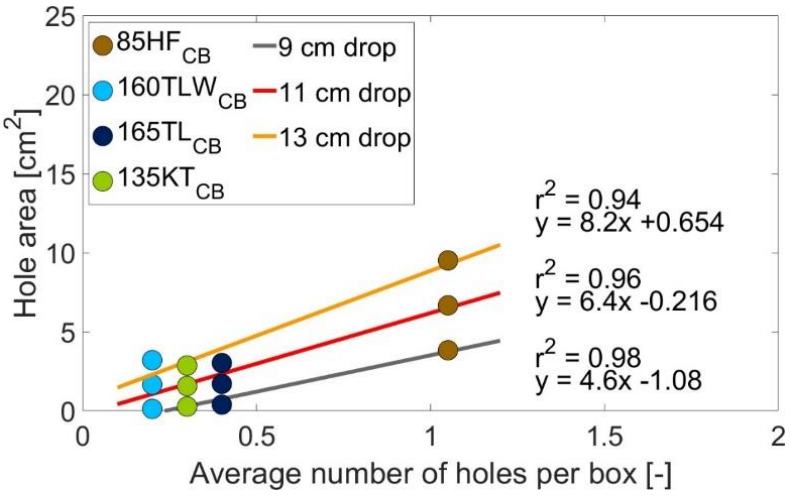

Fig. 14. Calculated hole areas plotted against the number of holes per box for three different drop heights

DISCUSSION

Designing packages for e-commerce and similar parcel distribution chains presents a complex challenge due to the variability of hazards encountered during transit. This work shows how a parameter can be established that connects the requirements from distribution chain hazards with the corrugated board box and its material. This parameter can be used to optimize packaging materials against penetrative hazards.

The proposed method has two main parts. The first part is to map the distribution chain using accelerometers and convert the data into cumulative distribution functions of

peak accelerations. The second part is to utilize previously published equations describing the energy absorbed by a corrugated board panel when penetrated by an impacting object. Eq. 3 is used to calculate puncture thresholds for the materials of interest, allowing the probability of damage to be determined from the CDFs. By assuming a drop height and using the box weight from the distribution chain mapping, Eq. 2 is employed to calculate theoretical hole areas for the same materials as the puncture thresholds. The probability of damage values and the calculated hole areas are then fitted by linear regression. The regression line is adjusted by changing the drop height to pass through the origin, defining a characteristic drop height for further optimization or material selection.

The characteristic drop height defined through this procedure is valid for single-wall corrugated board materials, provided the box size, total weight of the box, cushioning, and distribution chain remain the same. If the result from Fig. 8 is general, indicating that peak acceleration CDFs coincide between materials, it may not be necessary to use the same material data for calibration as for the corrugated boards used for distribution chain mapping. Instead, another set of well-characterized materials could be used to calibrate the characteristic drop height, for instance those presented in this work. This facilitates the possibility to map distribution chains without the need to first characterize the materials, and also to use data from already mapped distribution chains, provided the mappings have established a stable CDF. If the box weight is changed from the one used during mapping of the distribution chain and during the drop height calibration, a new characteristic drop height must be defined by recalculating the regression lines. However, it remains to be determined how much changes in cushioning or box weight would affect the acceleration CDFs in Fig. 11 or the acceleration-to-drop-height curve in Fig. 9. It is surmised that as long as the assumptions leading to Eq. 7 hold, minor weight or cushioning changes may not significantly affect the results. If a measured acceleration changes due to increased weight causing compression of the box or cushioning, this would be compensated by a corresponding but opposite change in distance over which the acceleration acts, for the same drop height. Nonetheless, it is known that boxes of different weights can be treated differently in the distribution chain (Böröcz and Németh 2025). For small packages and moderate weight changes, the differences may still be considered small for engineering purposes.

The proposed optimization technique utilizes material data and calculations, but alternative approaches are possible if experimental evidence is preferred. If the puncture threshold, defined by a previously determined characteristic drop height, is known, comparative performance evaluations can be conducted without extensive transport trials. For direct measurements, standardized tests such as ASTM D6344 or the concentrated impact test within ISTA 3B can be employed, provided the pendulum weight and/or drop height align with the puncture threshold for the intended box panel area (ASTM 2017; ISTA 3B 2017). This facilitates the optimization or quality control of corrugated board performance even in the absence of specific linerboard data. A drop with the pendulum should not cause a hole in the material if it is dropped with an energy level at, or below, the limiting puncture threshold.

CONCLUSIONS

1. The validity of a previously published design equation for blunt impacts with corrugated board in parcel deliveries has been demonstrated through field transport trials. The study showed that the equation correlated better with damage levels, as evaluated according to a known protocol, than burst strength or box compression strength.
2. The results indicate that a distribution chain can be characterized by a single parameter, denoted the characteristic drop height. This parameter can be used as a limiting design criterion to avoid or mitigate holes in the package.
3. The limiting criterion should be matched with another parameter described in this study, referred to as the puncture threshold of a material, which should be greater than the potential energy corresponding to the characteristic drop height in a free fall.
4. Once established, the characteristic drop height can be used to optimize single wall corrugated board against puncturing damages for packages within that distribution chain. The necessary data for this optimization are routinely measured properties. By utilizing this design method, time-consuming laboratory trials can be minimized, or eliminated, and the optimization finalized before the corrugated board is produced.

ACKNOWLEDGMENTS

The authors would like to acknowledge Thomas Ferge at DS Smith for his assistance with shipping boxes and visual evaluation. We are also grateful to DS Smith for supplying the paper and board materials used in this work.

REFERENCES CITED

Anon. (1919). "Lamp manufacturers see box tests at Forest Products Laboratory," *Fibre Containers* 4(3), 12.

ASTM D6344-04 (2017). "Standard test method for concentrated impacts to transport packages," ASTM International, West Conshohocken, PA, USA.

Batelka, J. J. (1994). *Corrugating Medium: Its Influence on Box Plant Operations and Combined Board Properties and Package Performance* (Project 3808), IPST, Atlanta.

Pitney Bowes Inc. (2023). *The Pitney Bowes Parcel Shipping Index 2023*, Stamford, CT, USA.

Browder, G. R. (1935). "A story of the fibre box and history of its developments," *Fibre Containers and Paperboard Mills* 20(8).

Buchanan, J. S. (1967). "Laboratory tests and corrugated case performance," *Boxboard Containers*, 75(4).

Böröcz, P. (2018). "Averaged vibration levels during courier parcel delivery service in small truck in Hungary," *FME Transactions* 46(2), 211-217. DOI: 10.5937/fmet1802211B

Böröcz, P., and Németh, Z. (2025). "Review paper on the field measurement of parcel packaging drop for testing purposes," *Packag Technol and Sci*. DOI: 10.1002/pts.2875

CCB (2022). "Cepi ContainerBoard list of grades: European list of corrugated base papers," (https://www.cepi-containerboard.org/download.php),accessed 4 april 2025.
Coffin, D. W. (2020). "Historical perspectives of corrugated box testing for 2020," *TAPPI J*. 19(3), 161-173.
FEFCO (1997). "TM 50 - Determination of the compression resistance of corrugated fibreboard containers," (https://www.fefco.org/), accessed 4 April 2025.
Harrod, S (2019). "E-commerce Packaging" as presented at the E-pack Europe, E-pack Europe, Berlin (https://www.smithers.com/home), accessed 4 April 2025.
Holmvall, M., Holmgren, M., and Rosdahl, M. (2024). "Designing corrugated board properties to mitigate puncturing impacts occurring in e-commerce or other demanding parcel handling distribution chains," *Packag Technol and Sci*. 37(10), 1017-1033. DOI: 10.1002/pts.2837
ISO 2759 (2014). "Board — Determination of bursting strength. International," Organization for Standardization, Geneva, Switzerland.
ISTA 3A (2018). "3A Packaged-products for parcel delivery system shipment 70 kg (150lb) or less," International Safe Transit Association, East Lansing, MI, USA.
ISTA 3B (2017). "3B Packaged-products for less-than-truckload (LTL) shipment," International Safe Transit Association, East Lansing, MI, USA.
ISTA 6-Amazon (2018). "Ships in own container (SIOC) for Amazon.com distribution system shipment," International Safe Transit Association, East Lansing, MI, USA.
Jönson, G. (1974). *Economy and Product Protection of Corrugated Board Containers*, Ph. D. Dissertation, Chalmers University of Technology, Göteborg.
Jönson, G. (1999). "Corrugated board package design: Stacking," in: *Corrugated Board Packaging*, Pira International, Randalls Road, Leatherhead, Surrey.
Kellicutt, K. Q. (1960a). "Note No. 19: Drop-testing technique for boxes - Part I," *Package Engineering* 5(8), 110-111.
Kellicutt, K. Q. (1960b). "Note No. 20: Drop-testing technique for boxes - Part II," *Package Engineering* 5(9), 118-119.
Kellicutt, K. Q., and Landt, E. F. (1951). "Basic design data for use of fibreboard in shipping containers," *Fibre Containers and Paperboard Mills* 36(12).
Kellicutt, K. Q., and Landt, E. F. (1956). "Strength evaluations of corrugated containers by the drop test method," *TAPPI J*. 39(9).
Lamb, M. J., and Rouillard, V. (2017). "Static and dynamic strength of paperboard containers subjected to variations in climatic conditions," *Packag Technol and Sci*, 30(3), 103-114. DOI: 10.1002/pts.2285
Maltenfort, G. G. (1989). "Mullen vs puncture for corrugated," in: *Performance and Evaluation of Shipping Containers*, G. G. Maltenfort (Ed.), Jelmar Publishing Co., Inc., Plainview, NY, USA.
Molnár, B., and Böröcz, P. (2021). "Experimental comparison of field and accelerated random vertical vibration levels of stacked packages for small parcel delivery shipments," *Appl. Sci*. 11. DOI: 10.3390/app11072927
Mrówczynski, D., Gajewski, T., and Garbowski, T. (2023). "A simplified dynamic strength analysis of cardboard packaging subjected to transport loads," *Materials* 16(14), article 5131. DOI: 10.3390/ma16145131
MSR175_plus (2025). "Transportation Data Logger with GPS Tracking: MSR175plus for Shock and Climate," MSR Electronics GmbH, (https://www.msr.ch/en/product/transport-data-logger-gps-msr175plus/), Accessed 4 April 2025.

Rouillard, V., and Lamb, M. J. (2020). "Using the Weibull distribution to characterise road transport vibration levels," *Packag. Technol. and Sci*. 33(7), 255-266. DOI: 10.1002/pts.2503

Rouillard, V., Lamb, M. J., Lepine, J., Long, M., and Ainalis, D. (2021). "The case for reviewing laboratory-based road transport simulations for packaging optimisation," *Packag Technol and Sci*. 34(6), 339-351. DOI: 10.1002/pts.2563

Singh, S. P., Singh, J., Chiang, K. C., and Saha, K. (2010). "Measurement and analysis of 'small' packages in next-day air shipments," *Packag. Technol. and Sci.* 23(1), 1-9. DOI: 10.1002/pts.873

Smithers (2024). "The Future of E-commerce Packaging to 2029," Ohio, USA, (https://www.smithers.com/services/market-reports/packaging/the-future-of-e-commerce-packaging-to-2029), Accessed 4 April 2025.

Steadman, R. (2002). "Corrugated board," in: *Handbook of Physical Testing of Paper*, R. E. Mark, C. Habeger, J. Borch, and M. B. Lyne (eds.), CRC Press, Boca Raton, FL, USA.

Article submitted: April 4, 2025; Peer review completed: April 27, 2025; Revised version received: May 5, 2025; Accepted: May 9, 2025; Published: May 13, 2025.
DOI: 10.15376/biores.20.3.5377-5397